Pol. J. Environ. Stud. Vol. 31, No. 5 (2022), 4177-4187
DOI: *10.15244/pjoes/147843* ONLINE PUBLICATION DATE: 2022-06-06

Original Research

Aerosolization Potential of Fungal Spores from the Colony Growing on HVAC Ducts

Xian Li*

School of Civil Engineering and Architecture, Linyi University, Linyi 276000, China

Received: 29 October 2021
Accepted: 30 March 2022

Abstract

Fungal spores can be detached from the ventilation duct and then transmitted indoors. As airflow sweeps the ventilation duct, it may decelerate in the boundary layer, and the resulting spore detachment may vary according to the position of the fungal colony. This study investigated the aerosolization potential of *Aspergillus niger* spores from the inner surface of four typical ventilation ducts. The airflow near the duct surface was numerically solved to determine the local air speed distribution at the height of the growing fungi. The results revealed that the spores growing at the center of the rectangular duct surface were more easily aerosolized than that growing at the corner. When the inlet air speed was 5.00 m/s, the spores of the 4- and 10-day-old colonies could not be detached when the dimensionless displacements of the circular tube were larger than 0.27 and 2.43, respectively. The aerosolization potential of spores increased with the β value and the constriction angle of the reducer. The maximum value of the local dimensionless air speed for the contraction angle of 50° (4.5) was greater than that for the contraction angle of 20° (4.0). Such information is useful for indoor mold contamination control.

Keywords: fungal spore, HVAC, aerosolization potential, ventilation duct, indoor air quality

Introduction

Indoor fungal pollution has become an increasing concern [1, 2]. Fungi are closely related to the respiratory tract diseases of indoor occupants [3, 4]. Allergy, infection and inflammation caused by fungal exposure account for more than 30% of people's incidence rate [5]. Fungal exposure includes inhalation and skin exposure, primarily caused by aerosolized fungal spores or mycelial fragments [6].

Approximately 40% of the indoor fungal pollution originates from the heating, ventilating, and air conditioning (HVAC) system [7]. When nutrients are available and environmental conditions are suitable, microorganisms can multiply on the ventilation duct [8]. After the air conditioning system runs for a long time, a large amount of dust and fungal particles accumulate on the surface of the ventilation duct [9]. The dust can provide nutrients for the growth of fungi. In addition, the temperature and humidity in the ventilation duct are benign for reproduction of fungi [10]. The concentration of dust accumulated fungi on the bottom of the return air duct was found to be as high as 8×10^5 CFU/g [11].

The aerosolization of fungal spores occurs when the external force exceeds the binding force between spores and the colony [12]. Take *Aspergillus*, one of the most common fungi in the indoor environment, as an example, its life cycle includes: spore germination, hypha formation and production of spore chain [13, 14].

*e-mail: lixian@lyu.edu.cn

For a spore chain, the junction between two adjacent spores is a septum. Because the septum is brittle, it is easy to be broken by external disturbances. The spores are then detached from the colony and form fungal aerosols [15].

The factors that affect the aerosolization of fungal spores can be divided into internal factors and environmental parameters. For the internal factor, the age of the colony has a significant impact on spore aerosolization [16]. As the colony grows, the septum between two spores becomes brittle and is then broken more easily. The force required to detach spores of the older colony is smaller than that of the younger colony [17]. Hence, the spore release potential for the older colony is higher than that for the younger colony.

For the environmental parameter, airflow is the main factor that drives the aerosolization of fungal spores [18]. As the blowing air speed increases, the drag force exerted on the spores becomes greater. The quantity of released spores was found to be positively correlated with the air speed from 1.7 m/s to 10 m/s [19]. The airflow generated by footsteps was considered to be the main reason for the detachment of microbial particles from the floor material [20]. Gusts, which have higher turbulence intensity, have better promotion in spore aerosolization [21].

Note that when airflow sweeps the inner surface of a ventilation duct, a boundary layer forms and then develops continuously with the flow development [22]. The height of a fungal colony is usually a few millimeters, and the colony is prone to fall into the boundary layer. Because the local air speed inside the boundary layer varies with the flow development, the drag forces on spores at different positions on the inner surface also vary. Spore detachment then varies with the growing position of the colony on the ventilation duct subjected to the airflow.

The above review shows that fungal spores can be aerosolized from the ventilation duct, and the age of colony and the air speed have significant impacts on spore aerosolization. Up to now, the differences in the aerosolization potential of spores from different positions on a ventilation duct remain unknown. This study investigated the aerosolization potential of fungal spores at different positions on the inner surface for four typical ventilation ducts. Both experimental tests and numerical simulations have been applied to investigate the aerosolization potential of fungal spores. The local airflow near the duct was numerically solved in order to compare the air speed distribution at the spores for the colony with the threshold speed to detach spores at different ages.

Materials and Methods

In this section, the schematic of the aerosolization tests of fungal spores is presented first, followed by the numerical simulation of airflow in the ventilation duct to obtain the local air speed distribution at the height of the growing fungi. The experimental test is used to estimate the correctness of the numerical modeling.

Experimental Study

For the experimental study, the rectangular duct was adopted to investigate the aerosolization potential of fungal spores from the duct. The fungal colony was exposed by the airflow in a wind tunnel, as illustrated in Fig. 1. The wind tunnel was composed of a centrifugal fan, a high efficiency particulate air (HEPA) filter, a ventilation duct, and an exhaust filter. After incubation, a fungal colony was placed at the center or corner (2 mm away from the side surface) of the bottom surface of the rectangular duct. The air was forced through the HEPA filter by the centrifugal fan, and the clean air swept the colony. The air speed could be adjusted by regulation of the electric frequency to the fan. The speed values ranged from 0.5 to 12 m/s and were measured by a hot-wire anemometer (Model VT110; KIMO Corp., France) with the resolution of 0.01m/s. Some of fungal spores were detached from the colony and were then collected by a sterile glass slide located downstream from the colony. The exhaust filter was used to collect airborne spores in the wind tunnel to prevent contamination of the indoor air.

The *Aspergillus niger* (*A. niger*) is one of the indicator fungi for indoor fungal contamination, and thus this study chose *A. niger* as the test fungal species [23]. To ensure the experiment was accurate, a pure species (CICC, 2089) was obtained from the Center of Industrial Culture Collection, China. Approximately 0.5 mL of the spore suspension with a concentration of 10^6 spores/mL was uniformly inoculated on the Sabouraud dextrose agar (SDA) plate. The incubation temperature for the test colony was 28ºC and the relative humidity was close to 100%. The incubation time of the test colony was seven days. The detailed cultivation method of the *A. niger* colony was reported in our previous study [17]. The spore density of the test colony was $(4.15\pm0.79) \times 10^6$ CFU/cm^2 based on five repeated measurements. The dimensions of the test colony were 5 mm × 5 mm.

The rectangular duct had a length of 150 cm, and the cross-sectional area was 30 cm × 30 cm. Honeycombs were installed at the inlet of the rectangular duct to make the inlet airflow uniformly. The honeycombs had a cell size of 3.175 mm and the thickness was 25.4 mm. The microscope slide was vertically installed 3.5 cm downstream from the colony. This value was the shortest distance from the colony, which the flow field at the position of the test colony was almost not influenced by the microscope slide based on the computational fluid dynamics (CFD) simulation. The dimensions of the microscope slide were 26 mm × 76 mm. To ensure the released spores adhere to the glass slide, Tween 20 was coated on the surface of the glass slide. Tween

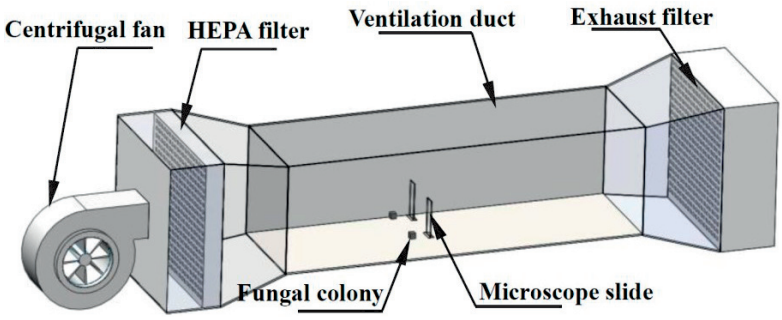

Fig. 1. Schematic diagram of wind tunnel for fungal spore aerosolization.

20 is a liquid surfactant that is viscous and soluble in water. Before each aerosolization test, it was uniformly smeared to the surface of the microscope slide by the sterile swab. The collected spores were suspended in the sterile water, and the spore suspension was then inoculated onto SDA plates to quantify the collected spores. Each experiment lasted 5 min. The results were reported as the spore release rate (CFU/(cm^2 min)).

Before each experiment, the ventilation duct was sprayed by 70% ethanol and purged by HEPA-filtered air, until the spore count was zero. Each test for a specific location was repeated five times. The inlet air speed in the rectangular duct was 5 m/s. The temperature and relative humidity inside the rectangular duct were 16-18ºC and 30-35%, respectively. Testing data were statistically analyzed using ANOVA model. Differences of $P<0.05$ were considered statistically significant [24].

CFD Modeling

Except for the experimental test, the numerical simulation was also applied to estimate the aerosolization potential of fungal spores. The simulated results for the rectangular duct were compared with the experimental data to validate the numerical simulation methodologies. In addition, another three typical air ducts, i.e., circular duct, elbow and reducer, were further investigated to estimate the spore aerosolization potential from the duct surface. Fig. 2 shows the three-dimensional physical model of the four typical air ducts commonly used in the HVAC system. The length of the circular and rectangular ducts was 5 m. The inner diameter of the circular duct was 0.3 m, and the cross-sectional dimensions of the rectangular duct were 0.3 m × 0.3 m. For the elbow, the bending angle of 90º was adopted, as shown in Fig. 2c). The β values of the ratio of the curvature radius (R) to the inner diameter (D) of the elbow were 1.0 and 1.5. Six representative positions in the elbow were adopted to estimate the air speed distribution at the height of the growing fungi. For the reducer, the contraction angles (θ) were 20º and 50º. The inner diameters of the duct before and after contraction were 0.3 m and 0.15 m, respectively.

Hexahedral grid cells were generated by a commercial preprocessing software program, integrated computer

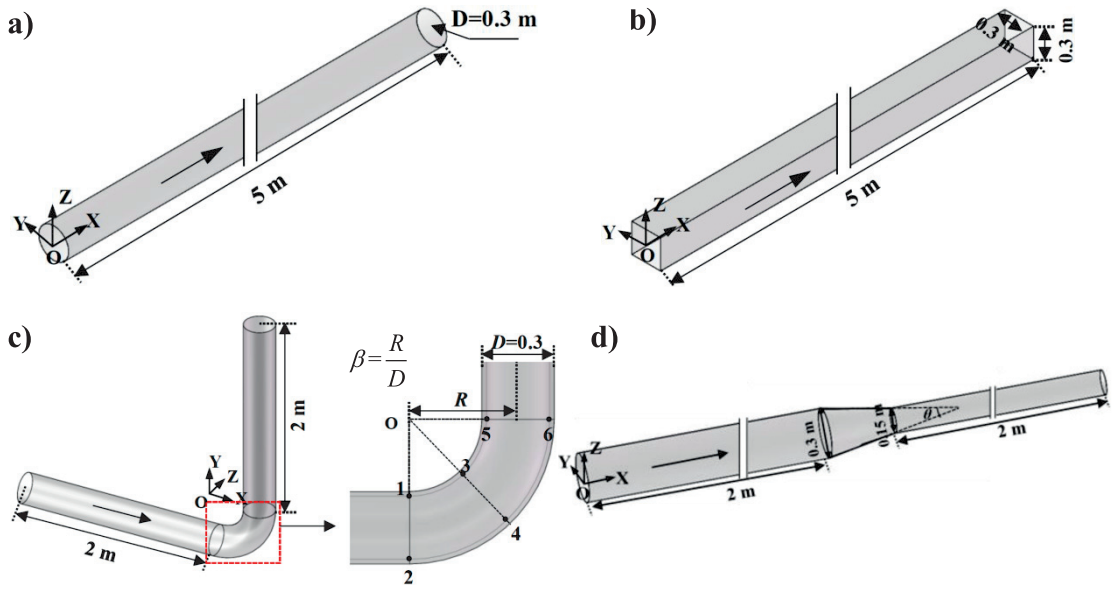

Fig. 2. Physical models of four typical air duct: a) circular duct; b) rectangular duct; c) elbow; d) reducer.

engineering and manufacturing (ICEM) (version 18.0.0). The average grid size for the four air ducts was approximately 5.7 mm. The grid cells near the solid wall were refined to capture the near-wall effect. All the y^+ values of the first near-wall grid cells were less than five. In order to verify that the grid size meets the requirements of grid independence, the grids were refined and enlarged, and new grid sizes of 4.8 mm and 6.9 mm were generated. The distribution of the local air speed near the duct wall was compared for the three grid sizes.

To assess the aerosolization potential of fungal spores, the air speed distribution at the height of the spores for the colony on the duct wall was solved by CFD. The core task of the numerical simulation was to solve the continuity, momentum and turbulence equations of fluid flow. The general scalar format can be summarized as:

$$\frac{\partial}{\partial t}(\rho\phi)+\frac{\partial}{\partial x_j}(\rho u_j\phi)=\frac{\partial}{\partial x_j}\left(\Gamma_{\phi,\text{eff}}\frac{\partial\phi}{\partial x_j}\right)+S_\phi \quad (1)$$

where ρ is the air density, φ is a scalar variable, t is time, u_j is the velocity component in three directions (x_j, j = 1, 2, 3) of the Cartesian coordinate system, $\Gamma_{\varphi,\text{eff}}$ is the effective diffusion coefficient, and S_φ is the source term. By varying φ, Equation (1) can be used to represent the continuity, momentum and turbulence equations. In this simulation, the air temperature in the ventilation duct was basically constant, thus, the energy equation was not resolved.

The boundary conditions for CFD simulations are shown in Table 1. The inlet boundary was set as velocity inlet, and the outlet boundary was free flow outlet. This study adopted the typical air speeds ranged from 3 m/s to 6 m/s as the inlet air speeds. According to the above air speed values, the airflow inside the air duct was turbulent. The renormalization group (RNG) k-ε model was used for turbulence simulation. Previous study has compared a set of eddy-viscosity models and concluded that the simulation results for the RNG k-ε model were closest to the experimental data [25].

In order to resolve the viscosity-affected region of the boundary layer, the enhanced wall treatment was adopted. The wall boundary was treated as a no-slip condition for flow. The pressure and velocity were coupled by the semi-implicit method for pressure linked equations (SIMPLE) algorithm. The convergence of numerical calculation was completed when the relative residuals were less than 1.0×10^{-5}. This study adopted the commercial CFD software, Fluent (version 18.0.0; ANSYS Corp., USA), to conduct the simulation work.

Table 1. Boundary conditions for CFD simulations.

Item	Value
Inlet boundary	Velocity inlet
Inlet air speed	3 m/s - 6 m/s
Exit boundary	Free flow outlet
y^+ values of the first near-wall grid cells	<5
Turbulence model	RNG k-ε model
Wall treatment	Enhanced wall treatment
Wall boundary of fluid	No-slip condition
Discretization scheme	Second-order upwind
Pressure and velocity coupling	SIMPLE algorithm

Results

Grid Size Independence Analysis

Table 2 presents the local dimensionless air speed (U/U_0) at the six representative positions of the elbow with the β value of 1.0 when the inlet air speed was 6.00 m/s. Where U is the local air speed at the height of the spores (m/s), U_0 is the inlet air speed of the circular duct (m/s). Here, the height of the *A. niger* colony was assumed to be 2 mm, because the colony height was measured as approximately 2 mm (in five repeated measurements) by an optical microscope. There was a little difference in the local dimensionless air speed between the three grid sizes, and the differences were within 5%. Therefore, the grid size of 5.7 mm was enough for the numerical investigation.

Spore Release Rate and Validation of Simulation and Measured Data

Fig. 3 shows the spore release rate of the *A. niger* colony at different positions on the bottom surface of the rectangular duct under the inlet air speed of 5.00 m/s. The spore release rate decreased with the dimensionless displacement (X/D). Where, X is the axial displacement of the circular duct (m), D is the inner diameter of the circular duct (m). The spore release rate at the center of the bottom surface for the dimensionless displacement of 2.0 was 6.44×10^3 CFU/(cm^2 min), while the release rate for the dimensionless displacement of 4.0 decreased to

Table 2. Local dimensionless air speed at the spores of six representative positions on the inner surface of the elbow under the inlet air speed of 6.00 m/s.

Average grid size (mm)	U/U_0					
	1	2	3	4	5	6
4.8	1.10	0.29	1.06	0.21	0.12	0.63
5.7	1.10	0.29	1.06	0.21	0.12	0.63
6.9	1.11	0.29	1.07	0.22	0.12	0.64

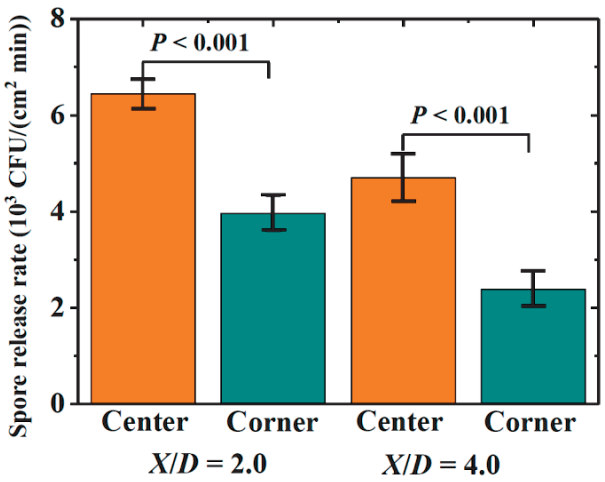

Fig. 3. Spore release rate of the colony at different positions on the bottom surface of the rectangular duct when the inlet air speed was 5.00 m/s, where error bars represent the standard deviations of five repeated experiments.

4.70 × 10^3 CFU/(cm^2 min). In addition, the spore release rate at the center of the bottom surface for the duct was significantly higher than that at the corner of the bottom surface (P<0.001). The results indicate that there was obvious dependence of the spore detachment on the growing position of the colony on the ventilation duct. There were significant differences in the local air speed at different positions of the duct surface due to the boundary layer. The profile of the local dimensionless air speed at the height of spores on the inner surface of the rectangular duct can be seen in Figs 6 and 7. The simulation results of the spore aerosolization potential were in accord with the experimental results, which indirectly illustrated the rationality of grid division, model selection and parameter settings in the CFD simulation.

Aerosolization Potential of Fungal Spores from the Ventilation Duct

After the numerical simulation was completed, the speed distribution of the airflow in the ventilation duct was known. The spore aerosolization potential was estimated by the profile of the local air speed at the height of fungal spores on the inner surface of the ventilation ducts.

Spore Aerosolization Potential on the Inner Surface of the Circular Duct

Fig. 4 shows the profile of the local dimensionless air speed at the height of *A. niger* spores on the inner surface of the circular duct under different inlet air speeds. The local dimensionless air speed decreased with the dimensionless displacement when the dimensionless value was less than 15. Fig. 5 presents the variation of the local dimensionless air speed with

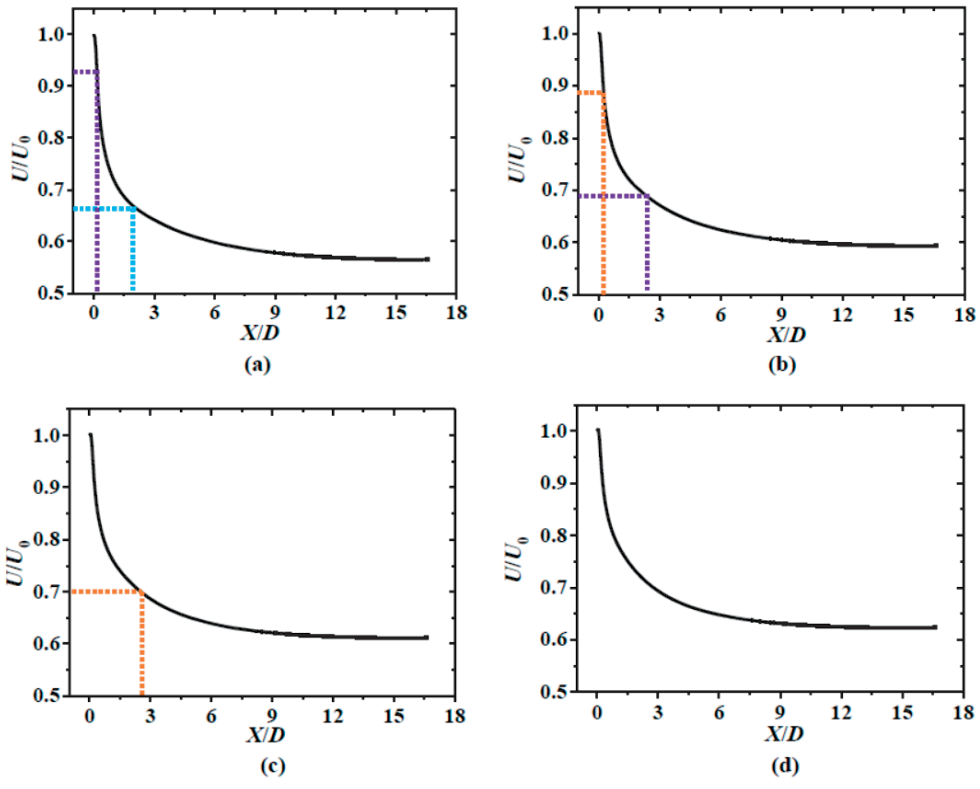

Fig. 4. Variation of the local dimensionless air speed (U/U_0) at the height of *A. niger* spores with the dimensionless displacement (X/D) under different inlet air speeds: a) 3.00 m/s; b) 4.00 m/s; c) 5.00 m/s; d) 6.00 m/s.

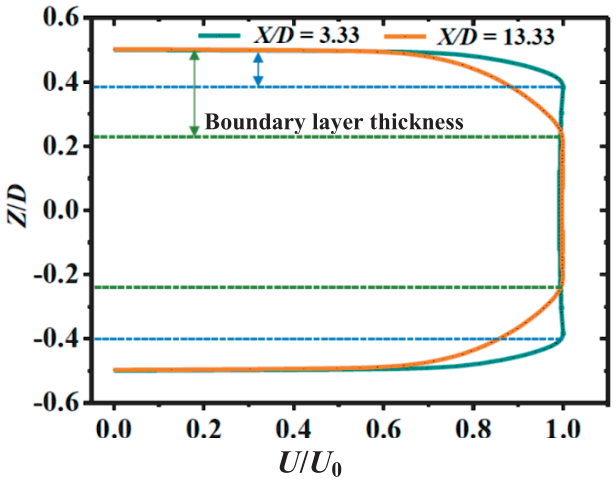

Fig. 5. Variation of the local dimensionless air speed (U/U_0) with the Z/D value at different dimensionless displacements (X/D) under the inlet air speed of 6.00 m/s.

the Z/D value at different dimensionless displacement values under the inlet air speed of 6.00 m/s. Where Z is the vertical distance from a certain position to the bottom surface of the duct (m). The nominal thickness of the boundary layer is the vertical distance from the outer edge of the boundary layer to the object surface. Generally, the position where the air speed reaches 99% of the mainstream speed is deemed as the outer edge of the boundary layer. The thickness of the boundary layer increased with the dimensionless displacement. In the boundary layer, the local dimensionless air speed decreased with the dimensionless displacement. The results indicate that the boundary layer had a significant effect on the local air speed at the spores of the colony and thus the spore aerosolization. The lower the dimensionless displacement, the easier it was for the detachment of fungal spores from the circular duct. The spores were detached more difficultly with the increase of the dimensionless displacement.

The profile of the local dimensionless air speed was compared with the threshold air speed for spore detachment of the *A. niger* colony at different ages. The threshold speed for spore detachment had been investigated in our pervious study [17]. The ages of the colony used for comparison were 4, 10, and 16 days, and the corresponding threshold air speeds were 3.50 m/s, 2.75 m/s and 2.00 m/s, respectively. In Fig. 4a), the local air speeds at the height of spores were 2.75 m/s and 2.00 m/s when the values of the dimensionless displacement were 0.17 and 1.90 under the inlet air speed of 3.00 m/s, respectively. Therefore, the colonies which were younger than 10 and 16 days could not be detached when the dimensionless displacements were larger than 0.17 and 1.90, respectively. Under the inlet air speed of 4.00 m/s, the spores of the 4-day-old and 10-day-old colonies could not be detached when the dimensionless displacements were larger than 0.27 and 2.43, respectively. When the inlet air speed reached to 5.00 m/s, the spores of the 4-day-old colony could not be detached when the dimensionless displacement was larger than 2.51. The results show that although the inlet air speed was higher than the threshold air speed for spore aerosolization of the *A. niger* colony at a certain age, the local air speed at the height of the spores might decrease below the threshold speed with the development of boundary layer. Significant aerosolization of spores would not be generated.

Spore Aerosolization Potential on the Inner Surface of the Rectangular Duct

Fig. 6 shows the variation of the local dimensionless air speed at the height of spores with the dimensionless displacement at different Y/D values for the rectangular duct under the inlet air speed of 6.00 m/s. Where D is the equivalent diameter of the rectangular duct which was four times the hydraulic radius, and the value was 0.3 m. The Y/D value was 0 meant that the colony was located at the center of the bottom surface of the rectangular duct, while the Y/D value was 0.493 meant that the colony was located at the corner of the bottom surface that was 2 mm away from the side surface. The simulation results of the air speed distribution at the height of spores under the Y/D value of 0 was consistent with that for the circular duct (Fig. 4), while the simulation results for the Y/D value of 0.493 had a large difference compared with the Y/D value of 0. When the Y/D value was 0.493, the local dimensionless air speed decreased more rapidly with the dimensionless displacement than that when the Y/D value was 0. For the same dimensionless displacement value, the local dimensionless air speed at the Y/D value of 0.493 was much lower than that at the Y/D value of 0. The above results indicate that the spores of the colony growing at the center of the rectangular duct surface were aerosolized more easily than that growing at the corner.

Fig. 7 indicates that due to the boundary layer, the local dimensionless air speed at the spores increased from the side surface of the rectangular duct to the center. In addition, the thickness of the boundary layer increased with the dimensionless displacement. The results show that the larger the dimensionless displacement, the more significant the effect of boundary layer on spore aerosolization from the inner surface of the rectangular duct.

Spore Aerosolization Potential on the Inner Surface of the Elbow Duct

Fig. 8 shows the velocity distribution of the airflow in the elbow duct when the β value was 1.0 under the inlet air speed of 3.00 m/s. In the bending section, the high-velocity zone was located on the inner side, and the low-velocity zone was located on the outer side. There was also a low-velocity zone at the posterior

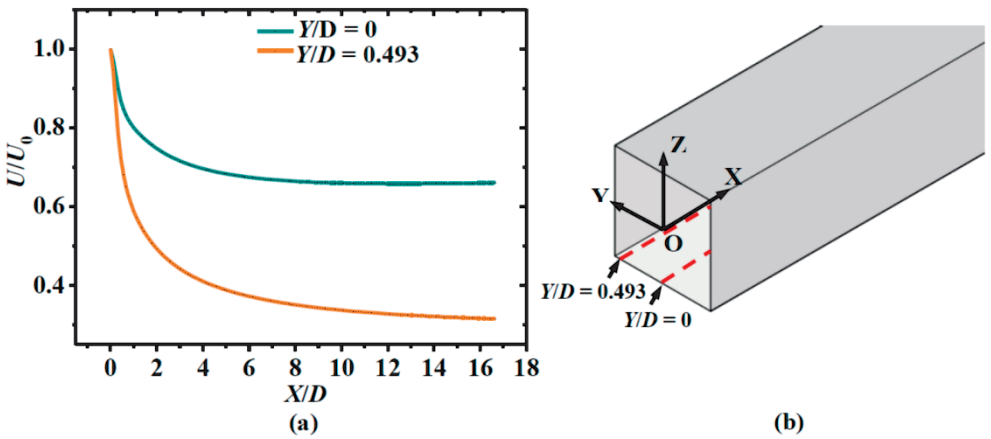

Fig. 6. Effect of the *Y/D* value on the air speed distribution at the height of the colony on the inner surface of the rectangular duct: a) variation of the local dimensionless air speed (U/U_0) with the dimensionless displacement (*X/D*) at different *Y/D* values under the inlet air speed of 6.00 m/s; b) schematic diagram of the location of the colony for different *Y/D* values.

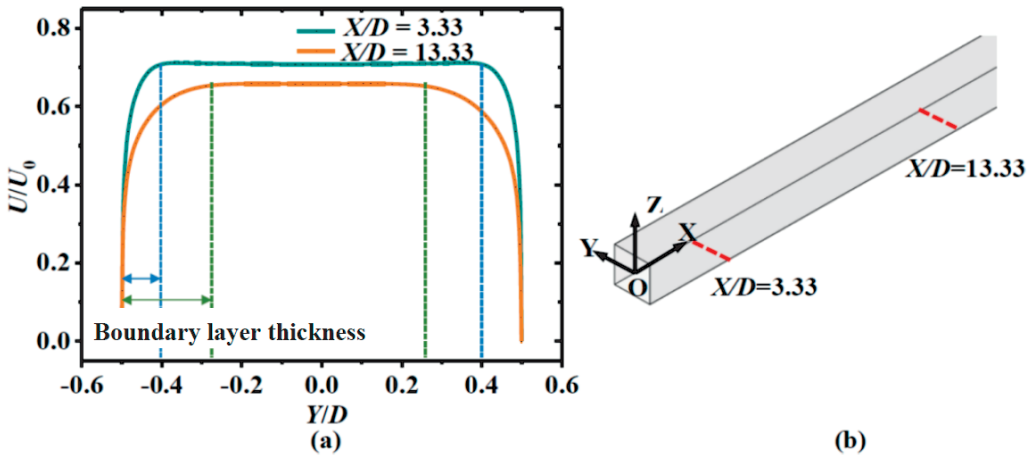

Fig. 7. Effect of the *Y/D* value on the air speed distribution at the height of the colony on the inner surface of the rectangular duct: a) variation of the local dimensionless air speed (U/U_0) with the *Y/D* value at different dimensionless displacement (*X/D*) values under the inlet air speed of 6.00 m/s; b) schematic diagram of the location of the colony for different dimensionless displacements.

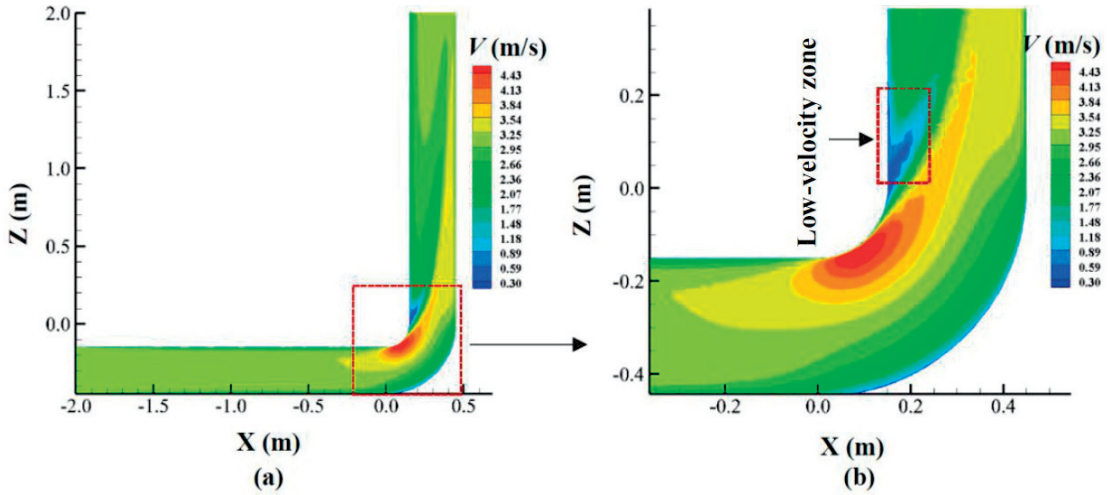

Fig. 8. Velocity distribution of the airflow in the elbow duct under the inlet air speed of 3.00 m/s when the β value was 1.0: a) planar view; b) local enlarged view of the dotted area of the elbow.

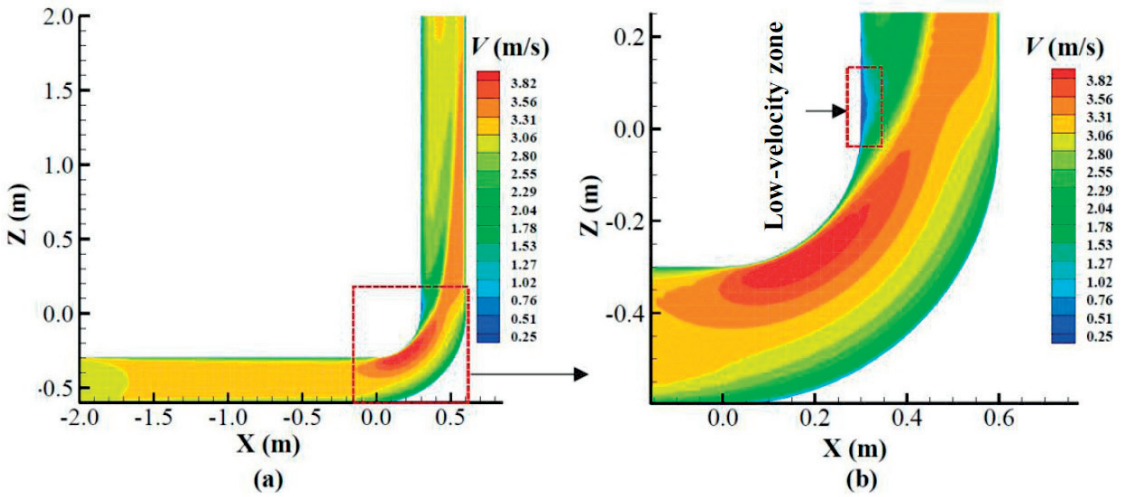

Fig. 9. Velocity distribution of the airflow in the elbow under the inlet air speed of 3.00 m/s when the β value was 1.5: a) planar view; b) local enlarged view of the dotted area of the bend.

of the inner side of the bending section, as shown in Fig. 8. The above showed that the spores of the colony growing on the inner side of the bending section were detached more easily than that on the outer side and at the posterior of the inner side. Fig. 9 presents the velocity distribution of the airflow in the elbow when the value of β was 1.5. Compared with Fig. 8, the range of the high-velocity zone in the elbow increased with the value of β. In addition, as the value of β increased, the low-velocity area at the posterior of the inner side of the bending section became smaller. Therefore, the spore release potential increased with the value of β.

Table 3 presents the simulation results of the local dimensionless air speed at the spores of six representative locations of the elbow (Fig. 2c)) when the value of β was 1.0. The local dimensionless air speeds at location 1 were all greater than 1.0. This indicates that the local air speed at the spores was greater than the inlet air speed, and the fungal spores therein were aerosolized more easily. While location 5 was in the low-velocity zone at the posterior of the bending section, thus the local air speed was lowest, and the fungal spores therein were aerosolized most difficultly.

Table 3. Local dimensionless air speeds at the spores of six representative locations on the inner surface of the elbow under different inlet air speeds when the β value was 1.0.

U_0 (m/s)	U/U_0					
	1	2	3	4	5	6
3.00	1.08	0.24	0.98	0.18	0.11	0.61
4.00	1.09	0.27	1.03	0.19	0.12	0.63
5.00	1.11	0.28	1.06	0.21	0.12	0.65
6.00	1.12	0.30	1.07	0.22	0.13	0.66

When the inlet air speed was 3.00 m/s, the local air speeds at locations 1 and 3 (3.24 and 2.94 m/s) exceeded the threshold air speed for spore detachment of the 10-day-old colony (2.75 m/s), while the local air speeds at locations 2, 4, 5 and 6 were all less than the threshold air speed of the 16-day-old colony (2.00 m/s). Thus, the spores of the 10-day-old colony at locations 1 and 3 could be aerosolized, while the spores of the 16-day-old colony at other four positions could not be detached. Similar results were obtained at other inlet air speeds. The results indicate that the local air speed at different positions of the elbow could differ greatly, which caused significant differences in the aerosolization potential of spores.

Spore Aerosolization Potential on the Inner Surface of the Reducer

Fig. 10 shows the distribution of the local dimensionless air speed at the spores on the inner surface of the reducer with different contraction angles. In the contraction section, the local dimensionless air speed increased rapidly with the dimensionless displacement. This was because the cross-sectional area of the duct became smaller. At the end of the contraction section, the local dimensionless air speed reached the maximum value, thus the fungal spores were detached most easily. After contraction, although the local dimensionless air speed gradually decreased with the dimensionless displacement, the local air speed had increased significantly compared with that before contraction.

In the contraction section, the larger the contraction angle, the faster the local dimensionless air speed increased with the dimensionless displacement. The maximum value of the local dimensionless air speed for the contraction angle of 50° (4.5) was greater than that for the contraction angle of 20° (4.0). After

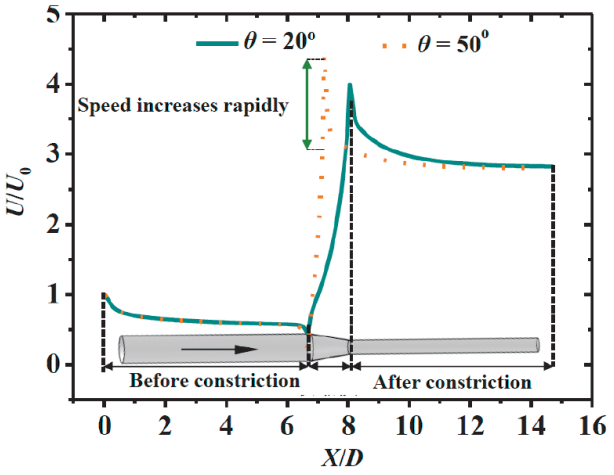

Fig. 10. Variation of the local dimensionless air speed (U/U_0) at the spores with the dimensionless displacement (X/D) at different contraction angles under the inlet air speed of 3.00 m/s.

contraction, the local dimensionless air speed for the lager contraction angle decreased more rapidly than that for the smaller contraction angle. The duct resistance increased with the contraction angle, and thus the air speed decreased. The above shows that the larger the contraction angle, the easier it was for fungal spores aerosolization from the contraction section, and the more difficult it was for that from the duct after contraction.

Discussion

Main Findings of this Study

The results indicate that the spore aerosolization potential varied greatly with the growing position of the colony on the ventilation duct in relation to the boundary layer. The potential of aerosolization of fungal spores from contaminated surfaces was assessed by Sivasubramani et al [26]. The spore release rate ranged from 10^2 to 10^3 cm^2/min, which was in accordance with the experimental results in this investigation. Previous literatures reported fungal contamination in the HVAC system. Bakker et al. quantified associations between microbial loads and air conditioning unit or building operational parameters [27]. Fungal concentrations varied among units, coil moisture, environmental and building characteristics with seven orders of magnitude. Fungal loads on copper surfaces in heat exchangers were found to be lower than on aluminum surfaces. However, there was not significant difference in the release of fungal spores between copper and aluminum heat exchangers [28]. Although previous literatures reported that fungal spores were released from the HVAC system into the air, no prior public reports have considered the effect of the local air speed on the spore aerosolization from the surface of the ventilation duct [7, 9, 11]. The great difference of the local air speed in proximity of the fungal spores at different positions of the ventilation duct were revealed in this study. Such information would contribute to the indoor mold contamination control.

Fig. 4 illustrates that the spore aerosolization potential decreases with the displacement. In order to minimize spore aerosolization, the ventilation duct shall maintain a large length instead of dividing into several short air ducts. Fig. 6 shows that the spores of the colony growing at the center surface of the rectangular duct are much easier to aerosolize than that growing at the corner. Hence, the center surface of the rectangular duct should be cleaned more often than the corner. Meanwhile, the spore release potential increased with the value of β for the elbow and the contraction angle for the reducer, as shown in Figs 8, 9 and 10. Low β value and contraction angle are the good choice for furnishing to prevent spores from detaching into the air. However, for ventilation duct cleaning, opposite strategies should be adopted. The above provides a general outline of the limited example application of the finding in this study.

Limitation of the Current Study and Outline of Future Research

Aerosolization of fungal spores is affected by fungal species. The difference can be explained by the structure of the colony [12]. The height of the conidiophore for *Aspergillus versicolor* (*A. versicolor*) is larger than that for *Cladosporium cladosporioides* (*C. cladosporioides*). Thus, the local air speed at the spores of *A. versicolor* is higher than that of *C. cladosporioides*. The spores of *A. versicolor* were thus easier to detach than that of *C. cladosporioides*. The findings of this study are only applicable for *A. niger*.

In this study, the growth substrate of the test colony was Sabouraud dextrose agar. The realistic environmental factors were not considered. To estimate spore release from general duct materials, other works need to be completed. A researcher may have to test the spore release rate of the colony growing on the general duct material. Nevertheless, one may use the results for a rough estimation, because spore aerosolization is mainly subject to the airflow.

For the aerosolization experiment, although the microscope slide spanned a certain area, some released spores might escape and were not collected by the microscope slide. Thus, the spore release rate might be underestimated. The aerodynamic diameter of the *A. niger* spores was approximately 3.2 μm. The collection efficiency of spores onto the microscope slide was approximately 93% based on relevant evaluation equations [29]. Further research is needed to measure the spore release rate more accurately.

In this study, the experimental test was used to estimate the correctness of the numerical modeling. The rectangular duct was taken as an example to illustrate the rationality of grid division, model

selection and parameter settings in the CFD simulation. The variation of the spore release rate with the growing position of the colony was in accordance with the profile of the local dimensionless air speed at the height of spores on the inner surface of the rectangular duct, which indirectly illustrates the rationality of the numerical modeling.

When the airflow swept the outer side of the bending section for the elbow (Figs 8 and 9), the angle of the erectly growing colony with the incoming airflow changed from 90º and 0º. The angle of 0º indicates that the colony was aligned with the upstream airflow, while the angle of 90º signifies that the colony was tangential to the upstream flow. For the angle of 90º, both drag and lift forces are among the major driving forces of spore detachment, while the impact force is the major driving force for the angle of 0º [26]. This study did not take into account the above variations. Further efforts are required to clarify these issues.

Conclusions

This study conducted the investigation of aerosolization potential of *Aspergillus niger* spores from the colony growing on the inner surface of the ventilation duct in relation to the boundary layer. Aerosolization tests and numerical simulations of the airflow in four typical ventilation ducts were performed to determine the air speed distribution at the height of spores and the spore release potential. It was found that the aerosolization potential of spores decreased with the development of the boundary layer in the circular and rectangular ducts. When the inlet air speed was 5.00 m/s, the spores of the 4- and 10-day-old colonies could not be detached when the dimensionless displacements of the circular tube were larger than 0.27 and 2.43, respectively. The spores of the colony growing at the center of the rectangular duct surface were aerosolized more easily than that growing at the corner. The local air speeds at different locations of the elbow could differ greatly, which caused significant differences in the spore aerosolization. When the inlet air speed was 3.00 m/s, the local air speeds at locations 1 and 3 (3.24 and 2.94 m/s) exceeded the threshold air speed for spore detachment of the 10-day-old colony (2.75 m/s), while the local air speeds at locations 2, 4, 5 and 6 were all less than the threshold air speed of the 16-day-old colony (2.00 m/s). The aerosolization potential of spores increased with the β value of the ratio of the curvature radius to the inner diameter of the elbow. The maximum value of the local dimensionless air speed for the contraction angle of 50º (4.5) was greater than that for the contraction angle of 20º (4.0). The larger the contraction angle, the easier it was for spore aerosolization from the contraction section of the reducer. Such information is useful for controlling the indoor mold contamination.

Acknowledgments

This work was supported by the Natural Science Foundation of Shandong Province, China (Grant No.: ZR2021QE027).

Conflict of Interest

The authors declare no conflict of interest.

References

1. FANG Z., TANG Q., GONG C., OUYANG Z., LIU P., SUN L., WANG, X. Profile and distribution characteristics of culturable airborne fungi in residential homes with children in Beijing, China. Indoor Built Environ., **26**, 1232, **2017**.
2. OSMAN M., IBRAHIM H.Y., YOUSEF F.A., ELNASR A.A., SAEED Y., HAMEED AA. A study on microbiological contamination on air quality in hospitals in Egypt. Indoor Built Environ., **27**, 953, **2017**.
3. WLAZŁO Ł., KASELA M., BOŻENA NOWAKOWICZ-DĘBEK B., OSSOWSKI M., MALM A. Bioaerosols in an underground tourist trail. Pol. J. Environ. Stud., **29**, 3865, **2020**.
4. EJDYS E., DYNOWSKA M., BIEDUNKIEWICZ A., SUCHARZEWSKA E. An overview of the species of fungi occurring in school rooms - a four-year study. Pol. J. Environ. Stud., **22**, 1691, **2013**.
5. KHAN A.A.H., KARUPPAYIL S.M. Fungal pollution of indoor environments and its management. Saudi J. Biol. Sci., **19**, 405, **2012**.
6. KWANA H., KUBERKA A. Fungi in public heritage buildings in Poland. Pol. J. Environ. Stud., **29**, 3651, **2020**.
7. LIU Z., MA S., CAO G., MENG C., HE B.J. Distribution characteristics, growth, reproduction and transmission modes and control strategies for microbial contamination in HVAC systems: A literature review. Energ. Buildings, **177**, 77, **2018**.
8. HUGENHOLTZ P., FUERST J.A. Heterotrophic bacteria in an air-handling system. Appl. Environ. Microbiol., **58**, 3914, **1992**.
9. WILSON S.C., PALMATIER R.N., ANDRIYCHUK L.A., MARTIN J.M., JUMPER C.A., HOLDER H.W., STRAUS D.C. Mold contamination and air handling units. *J. Occup. Environ. Hyg.*, **4**, 483, **2007**.
10. CHANG J.C.S., FOARDE K.K., VANOSDELL D.W. Assessment of fungal (*Penicillium chrysogenum*) growth on three HVAC duct materials. Environ. Int., **22**, 425, **1996**.
11. LI A., XIONG J., YAO L., GOU L., ZHANG W. Determination of dust and microorganism accumulation in different designs of AHU system in Shaanxi History Museum. Build. Environ., **104**, 232, **2016**.
12. GORNY R.L., REPONEN T., GRINSHPUN S.A., WILLEKE K. Source strength of fungal spore aerosolization from moldy building material. Atmos. Environ., **35**, 4853, **2001**.
13. KRIJGSHELD P., BLEICHRODT R., VAN V.G.J., WANG F., MÜLLER W.H., DIJKSTERHUIS J., WÖSTEN H.A.B. Development in *Aspergillus*. Stud. Mycol., **74**, 1, **2013**.

14. LI X., FU H. Fungal spore aerosolization at different positions of a growing colony blown by airflow. Aerosol. Air Qual. Res., **20**, 2826, **2020**.
15. KILDESO J., WURTZ H., NIELSEN K.F., KRUSE P., WILKINS K., THRANE U., GRAVESEN S., NIELSEN P.A., SCHNEIDER T. Determination of fungal spore release from wet building materials. Indoor Air, **13**, 148, **2003**.
16. TEERTSTRA W.R., TEGELAAR M., DIJKSTERHUIS J., GOLOVINA E.A., OHM R.A., WÖSTEN H.A. Maturation of conidia on conidiophores of *Aspergillus niger*. Fungal Genet. Biol., **98**, 61, **2017**.
17. LI X., ZHANG T., WANG S. Measuring detachment of *Aspergillus niger* spores from colonies with an atomic force microscope. Indoor Air, **28**, 744, **2018**.
18. GOPALAKRISHNAN S., ARIGELA R., GUPTA S.K., RAGHUNATHAN R. Dynamic response of passive release of fungal spores from exposure to air. J. Aerosol Sci., **133**, 37, **2019**.
19. ZOBERI M.H. Take-off of mould spores in relation to wind speed and humidity. Ann. Bot., **25** (1), 53, **1961**.
20. KHARE P., MARR L.C. Simulation of vertical concentration gradient of influenza viruses in dust resuspended by walking. Indoor Air, **25**, 428, **2015**.
21. WADIA K.D.R, MCCARTNEY H.A., BUTLER D.R. Dispersal of *Passalora personata* conidia from groundnut by wind and rain. Mycol. Res., **102**, 355, **1998**.
22. KANG H., YOO J. Turbulence characteristics of the three-dimensional boundary layer on a rotating disk with jet impingement. Exp. Fluids, **33**, 270, **2002**.
23. LIU Z., ZHU Z., ZHU Y., XU W., LI H. Investigation of dust loading and culturable microorganisms of HVAC systems in 24 office buildings in Beijing. Energ. Buildings, **103**, 166, **2015**.
24. MENSAH-ATTIPOE J., SAARI S., VEIJALAINEN A.M., PASANEN P., KESKINEN J., LESKINEN, J. Release and characteristics of fungal fragments in various conditions. Sci. Total Environ., **547**, 234, **2016**.
25. CHEN Q. Comparison of different k-epsilon models for indoor air-flow computations. Numer. Heat Tr. B-fund., **28**, 353, **1995**.
26. SIVASUBRAMANI S.K., NIEMEIER R.T., REPONEN T., GRINSHPUN, S.A. Assessment of the aerosolization potential for fungal spores in moldy homes. Indoor Air, **14**, 405, **2004**.
27. BAKKER A., SIEGEL J.A., MENDELL M.J., PECCIA J. Building and environmental factors that influence bacterial and fungal loading on air conditioning cooling coils. Indoor Air, **28**(5), 689, **2018**.
28. FEIGLEY C., KHAN J., SALZBERG D., HUSSEY J., ATTAWAY H., STEED L., SCHMIDT M., MICHELS H. Experimental tests of copper components in ventilation systems for microbial control. HVAC&R. Res., **19**(1), 53, **2013**.
29. HINDS W.C. Aerosol technology: properties, behavior, and measurement of airborne particles. 2nd ed. Los Angeles: Wiley, 20, **1999**.